

Search for CP violation using T -odd correlations in $D^+ \rightarrow K^+ K_S^0 \pi^+ \pi^-$ and $D_s^+ \rightarrow K^+ K_S^0 \pi^+ \pi^-$ decays

J. P. Lees,¹ V. Poireau,¹ V. Tisserand,¹ J. Garra Tico,² E. Grauges,² M. Martinelli,^{3a,3b} D. A. Milanes,^{3a} A. Palano,^{3a,3b} M. Pappagallo,^{3a,3b} G. Eigen,³ B. Stugu,³ L. Sun,³ D. N. Brown,⁴ L. T. Kerth,⁴ Yu. G. Kolomensky,⁴ G. Lynch,⁴ H. Koch,⁵ T. Schroeder,⁵ D. J. Asgeirsson,⁶ C. Hearty,⁶ T. S. Mattison,⁶ J. A. McKenna,⁶ A. Khan,⁷ V. E. Blinov,⁸ A. R. Buzykaev,⁸ V. P. Druzhinin,⁸ V. B. Golubev,⁸ E. A. Kravchenko,⁸ A. P. Onuchin,⁸ S. I. Serednyakov,⁸ Yu. I. Skovpen,⁸ E. P. Solodov,⁸ K. Yu. Todyshev,⁸ A. N. Yushkov,⁸ M. Bondioli,⁹ D. Kirkby,⁹ A. J. Lankford,⁹ M. Mandelkern,⁹ D. P. Stoker,⁹ H. Atmacan,¹⁰ J. W. Gary,¹⁰ F. Liu,¹⁰ O. Long,¹⁰ G. M. Vitug,¹⁰ C. Campagnari,¹¹ T. M. Hong,¹¹ D. Kovalskyi,¹¹ J. D. Richman,¹¹ C. A. West,¹¹ A. M. Eisner,¹² J. Kroseberg,¹² W. S. Lockman,¹² A. J. Martinez,¹² T. Schalk,¹² B. A. Schumm,¹² A. Seiden,¹² C. H. Cheng,¹³ D. A. Doll,¹³ B. Echenard,¹³ K. T. Flood,¹³ D. G. Hitlin,¹³ P. Ongmongkolkul,¹³ F. C. Porter,¹³ A. Y. Rakitin,¹³ R. Andreassen,¹⁴ M. S. Dubrovin,¹⁴ B. T. Meadows,¹⁴ M. D. Sokoloff,¹⁴ P. C. Bloom,¹⁵ W. T. Ford,¹⁵ A. Gaz,¹⁵ M. Nagel,¹⁵ U. Nauenberg,¹⁵ J. G. Smith,¹⁵ S. R. Wagner,¹⁵ R. Ayad,^{16,*} W. H. Toki,¹⁶ B. Spaan,¹⁷ M. J. Kobel,¹⁸ K. R. Schubert,¹⁸ R. Schwierz,¹⁸ D. Bernard,¹⁹ M. Verderi,¹⁹ P. J. Clark,²⁰ S. Playfer,²⁰ D. Bettoni,^{22a} C. Bozzi,^{22a} R. Calabrese,^{22a,22b} G. Cibinetto,^{22a,22b} E. Fioravanti,^{22a,22b} I. Garzia,^{22a,22b} E. Luppi,^{22a,22b} M. Munerato,^{22a,22b} M. Negrini,^{22a,22b} L. Piemontese,^{22a} R. Baldini-Ferroli,²¹ A. Calcaterra,²¹ R. de Sangro,²¹ G. Finocchiaro,²¹ M. Nicolaci,²¹ P. Patteri,²¹ I. M. Peruzzi,^{21,†} M. Piccolo,²¹ M. Rama,²¹ A. Zallo,²¹ R. Contri,^{24a,24b} E. Guido,^{24a,24b} M. Lo Vetere,^{24a,24b} M. R. Monge,^{24a,24b} S. Passaggio,^{24a} C. Patrignani,^{24a,24b} E. Robutti,^{24a} B. Bhuyan,²² V. Prasad,²² C. L. Lee,²³ M. Morii,²³ A. J. Edwards,²⁴ A. Adametz,²⁵ J. Marks,²⁵ U. Uwer,²⁵ F. U. Bernlochner,²⁶ M. Ebert,²⁶ H. M. Lacker,²⁶ T. Lueck,²⁶ P. D. Dauncey,²⁷ M. Tibbetts,²⁷ P. K. Behera,²⁸ U. Mallik,²⁸ C. Chen,²⁹ J. Cochran,²⁹ W. T. Meyer,²⁹ S. Prell,²⁹ E. I. Rosenberg,²⁹ A. E. Rubin,²⁹ A. V. Gritsan,³⁰ Z. J. Guo,³⁰ N. Arnaud,³¹ M. Davier,³¹ G. Grosdidier,³¹ F. Le Diberder,³¹ A. M. Lutz,³¹ B. Malaescu,³¹ P. Roudeau,³¹ M. H. Schune,³¹ A. Stocchi,³¹ G. Wormser,³¹ D. J. Lange,³² D. M. Wright,³² I. Bingham,³³ C. A. Chavez,³³ J. P. Coleman,³³ J. R. Fry,³³ E. Gabathuler,³³ D. E. Hutchcroft,³³ D. J. Payne,³³ C. Touramanis,³³ A. J. Bevan,³⁴ F. Di Lodovico,³⁴ R. Sacco,³⁴ M. Sigamani,³⁴ G. Cowan,³⁵ S. Paramesvaran,³⁵ D. N. Brown,³⁶ C. L. Davis,³⁶ A. G. Denig,³⁷ M. Fritsch,³⁷ W. Gradl,³⁷ A. Hafner,³⁷ E. Prencipe,³⁷ K. E. Alwyn,³⁸ D. Bailey,³⁸ R. J. Barlow,³⁸ G. Jackson,³⁸ G. D. Lafferty,³⁸ R. Cenci,³⁹ B. Hamilton,³⁹ A. Jawahery,³⁹ D. A. Roberts,³⁹ G. Simi,³⁹ C. Dallapiccola,⁴⁰ R. Cowan,⁴¹ D. Dujmic,⁴¹ G. Sciolla,⁴¹ D. Lindemann,⁴² P. M. Patel,⁴² S. H. Robertson,⁴² M. Schram,⁴² P. Biassoni,^{46a,46b} A. Lazzaro,^{46a,46b} V. Lombardo,^{46a} N. Neri,^{46a,46b} F. Palombo,^{46a,46b} S. Stracka,^{46a,46b} L. Cremaldi,⁴³ R. Godang,^{43,‡} R. Kroeger,⁴³ P. Sonnek,⁴³ D. J. Summers,⁴³ X. Nguyen,⁴⁴ P. Taras,⁴⁴ G. De Nardo,^{49a,49b} D. Monorchio,^{49a,49b} G. Onorato,^{49a,49b} C. Sciacca,^{49a,49b} G. Raven,⁴⁵ H. L. Snoek,⁴⁵ C. P. Jessop,⁴⁶ K. J. Knoepfel,⁴⁶ J. M. LoSecco,⁴⁶ W. F. Wang,⁴⁶ K. Honscheid,⁴⁷ R. Kass,⁴⁷ J. Brau,⁴⁸ R. Frey,⁴⁸ N. B. Sinev,⁴⁸ D. Strom,⁴⁸ E. Torrence,⁴⁸ E. Feltresi,^{54a,54b} N. Gagliardi,^{54a,54b} M. Margoni,^{54a,54b} M. Morandin,^{54a} M. Posocco,^{54a} M. Rotondo,^{54a} F. Simonetto,^{54a,54b} R. Stroili,^{54a,54b} E. Ben-Haim,⁴⁹ M. Bomben,⁴⁹ G. R. Bonneaud,⁴⁹ H. Briand,⁴⁹ G. Calderini,⁴⁹ J. Chauveau,⁴⁹ O. Hamon,⁴⁹ Ph. Leruste,⁴⁹ G. Marchiori,⁴⁹ J. Ocariz,⁴⁹ S. Sitt,⁴⁹ M. Biasini,^{56a,56b} E. Manoni,^{56a,56b} S. Pacetti,^{56a,56b} A. Rossi,^{56a,56b} C. Angelini,^{57a,57b} G. Batignani,^{57a,57b} S. Bettarini,^{57a,57b} M. Carpinelli,^{57a,57b,§} G. Casarosa,^{57a,57b} A. Cervelli,^{57a,57b} F. Forti,^{57a,57b} M. A. Giorgi,^{57a,57b} A. Lusiani,^{57a,57c} B. Oberhof,^{57a,57b} E. Paoloni,^{57a,57b} A. Perez,^{57a} G. Rizzo,^{57a,57b} J. J. Walsh,^{57a} D. Lopes Pegna,⁵⁰ C. Lu,⁵⁰ J. Olsen,⁵⁰ A. J. S. Smith,⁵⁰ A. V. Telnov,⁵⁰ F. Anulli,^{59a} G. Cavoto,^{59a} R. Faccini,^{59a,59b} F. Ferrarotto,^{59a} F. Ferroni,^{59a,59b} M. Gaspero,^{59a,59b} L. Li Gioi,^{59a} M. A. Mazzoni,^{59a} G. Piredda,^{59a} C. Büniger,⁵¹ O. Grünberg,⁵¹ T. Hartmann,⁵¹ T. Leddig,⁵¹ H. Schröder,⁵¹ R. Waldi,⁵¹ T. Adye,⁵² E. O. Olaiya,⁵² F. F. Wilson,⁵² S. Emery,⁵³ G. Hamel de Monchenault,⁵³ G. Vasseur,⁵³ Ch. Yèche,⁵³ D. Aston,⁵⁴ D. J. Bard,⁵⁴ R. Bartoldus,⁵⁴ C. Cartaro,⁵⁴ M. R. Convery,⁵⁴ J. Dorfan,⁵⁴ G. P. Dubois-Felsmann,⁵⁴ W. Dunwoodie,⁵⁴ R. C. Field,⁵⁴ M. Franco Sevilla,⁵⁴ B. G. Fulsom,⁵⁴ A. M. Gabareen,⁵⁴ M. T. Graham,⁵⁴ P. Grenier,⁵⁴ C. Hast,⁵⁴ W. R. Innes,⁵⁴ M. H. Kelsey,⁵⁴ H. Kim,⁵⁴ P. Kim,⁵⁴ M. L. Kocian,⁵⁴ D. W. G. S. Leith,⁵⁴ P. Lewis,⁵⁴ S. Li,⁵⁴ B. Lindquist,⁵⁴ S. Luitz,⁵⁴ V. Luth,⁵⁴ H. L. Lynch,⁵⁴ D. B. MacFarlane,⁵⁴ D. R. Muller,⁵⁴ H. Neal,⁵⁴ S. Nelson,⁵⁴ I. Ofte,⁵⁴ M. Perl,⁵⁴ T. Pulliam,⁵⁴ B. N. Ratcliff,⁵⁴ A. Roodman,⁵⁴ A. A. Salnikov,⁵⁴ V. Santoro,⁵⁴ R. H. Schindler,⁵⁴ A. Snyder,⁵⁴ D. Su,⁵⁴ M. K. Sullivan,⁵⁴ J. Va'vra,⁵⁴ A. P. Wagner,⁵⁴ M. Weaver,⁵⁴ W. J. Wisniewski,⁵⁴ M. Wittgen,⁵⁴ D. H. Wright,⁵⁴ H. W. Wulsin,⁵⁴ A. K. Yarritu,⁵⁴ C. C. Young,⁵⁴ V. Ziegler,⁵⁴ W. Park,⁵⁵ M. V. Purohit,⁵⁵ R. M. White,⁵⁵ J. R. Wilson,⁵⁵ A. Randle-Conde,⁵⁶ S. J. Sekula,⁵⁶ M. Bellis,⁵⁷ J. F. Benitez,⁵⁷ P. R. Burchat,⁵⁷ T. S. Miyashita,⁵⁷ M. S. Alam,⁵⁸ J. A. Ernst,⁵⁸ R. Gorodeisky,⁵⁹ N. Guttman,⁵⁹ D. R. Peimer,⁵⁹ A. Soffer,⁵⁹ P. Lund,⁶⁰ S. M. Spanier,⁶⁰ R. Eckmann,⁶¹ J. L. Ritchie,⁶¹ A. M. Ruland,⁶¹ C. J. Schilling,⁶¹

R. F. Schwitters,⁶¹ B. C. Wray,⁶¹ J. M. Izen,⁶² X. C. Lou,⁶² F. Bianchi,^{72a,72b} D. Gamba,^{72a,72b} L. Lanceri,^{73a,73b} L. Vitale,^{73a,73b} F. Martinez-Vidal,⁶³ A. Oyanguren,⁶³ H. Ahmed,⁶⁴ J. Albert,⁶⁴ Sw. Banerjee,⁶⁴ H. H. F. Choi,⁶⁴ G. J. King,⁶⁴ R. Kowalewski,⁶⁴ M. J. Lewczuk,⁶⁴ C. Lindsay,⁶⁴ I. M. Nugent,⁶⁴ J. M. Roney,⁶⁴ R. J. Sobie,⁶⁴ T. J. Gershon,⁶⁵ P. F. Harrison,⁶⁵ T. E. Latham,⁶⁵ E. M. T. Puccio,⁶⁵ H. R. Band,⁶⁶ S. Dasu,⁶⁶ Y. Pan,⁶⁶ R. Prepost,⁶⁶ C. O. Vuosalo,⁶⁶ and S. L. Wu⁶⁶

(BABAR Collaboration)

¹*Laboratoire d'Annecy-le-Vieux de Physique des Particules (LAPP), Université de Savoie, CNRS/IN2P3, F-74941 Annecy-Le-Vieux, France*

²*Universitat de Barcelona, Facultat de Física, Departament ECM, E-08028 Barcelona, Spain*

^{3a}*INFN Sezione di Bari, I-70126 Bari, Italy*

^{3b}*Dipartimento di Fisica, Università di Bari, I-70126 Bari, Italy*

³*University of Bergen, Institute of Physics, N-5007 Bergen, Norway*

⁴*Lawrence Berkeley National Laboratory and University of California, Berkeley, California 94720, USA*

⁵*Ruhr Universität Bochum, Institut für Experimentalphysik 1, D-44780 Bochum, Germany*

⁶*University of British Columbia, Vancouver, British Columbia, Canada V6T 1Z1*

⁷*Brunel University, Uxbridge, Middlesex UB8 3PH, United Kingdom*

⁸*Budker Institute of Nuclear Physics, Novosibirsk 630090, Russia*

⁹*University of California at Irvine, Irvine, California 92697, USA*

¹⁰*University of California at Riverside, Riverside, California 92521, USA*

¹¹*University of California at Santa Barbara, Santa Barbara, California 93106, USA*

¹²*University of California at Santa Cruz, Institute for Particle Physics, Santa Cruz, California 95064, USA*

¹³*California Institute of Technology, Pasadena, California 91125, USA*

¹⁴*University of Cincinnati, Cincinnati, Ohio 45221, USA*

¹⁵*University of Colorado, Boulder, Colorado 80309, USA*

¹⁶*Colorado State University, Fort Collins, Colorado 80523, USA*

¹⁷*Technische Universität Dortmund, Fakultät Physik, D-44221 Dortmund, Germany*

¹⁸*Technische Universität Dresden, Institut für Kern- und Teilchenphysik, D-01062 Dresden, Germany*

¹⁹*Laboratoire Leprince-Ringuet, Ecole Polytechnique, CNRS/IN2P3, F-91128 Palaiseau, France*

²⁰*University of Edinburgh, Edinburgh EH9 3JZ, United Kingdom*

^{22a}*INFN Sezione di Ferrara; I-44100 Ferrara, Italy*

^{22b}*Dipartimento di Fisica, Università di Ferrara, I-44100 Ferrara, Italy*

²¹*INFN Laboratori Nazionali di Frascati, I-00044 Frascati, Italy*

^{24a}*INFN Sezione di Genova; I-16146 Genova, Italy*

^{24b}*Dipartimento di Fisica, Università di Genova, I-16146 Genova, Italy*

²²*Indian Institute of Technology Guwahati, Guwahati, Assam, 781 039, India*

²³*Harvard University, Cambridge, Massachusetts 02138, USA*

²⁴*Harvey Mudd College, Claremont, California 91711, USA*

²⁵*Universität Heidelberg, Physikalisches Institut, Philosophenweg 12, D-69120 Heidelberg, Germany*

²⁶*Humboldt-Universität zu Berlin, Institut für Physik, Newtonstraße 15, D-12489 Berlin, Germany*

²⁷*Imperial College London, London, SW7 2AZ, United Kingdom*

²⁸*University of Iowa, Iowa City, Iowa 52242, USA*

²⁹*Iowa State University, Ames, Iowa 50011-3160, USA*

³⁰*Johns Hopkins University, Baltimore, Maryland 21218, USA*

³¹*Laboratoire de l'Accélérateur Linéaire, IN2P3/CNRS et Université Paris-Sud 11, Centre Scientifique d'Orsay, B.P. 34, F-91898 Orsay Cedex, France*

³²*Lawrence Livermore National Laboratory, Livermore, California 94550, USA*

³³*University of Liverpool, Liverpool L69 7ZE, United Kingdom*

*Now at Temple University, Philadelphia, PA 19122, USA.

†Also with Università di Perugia, Dipartimento di Fisica, Perugia, Italy.

‡Now at University of South Alabama, Mobile, AL 36688, USA.

§Also with Università di Sassari, Sassari, Italy.

||Also with Università della Basilicata, Potenza, Italy.

¶Also with Università di Sassari, Sassari, Italy.

- ³⁴*Queen Mary, University of London, London, E1 4NS, United Kingdom*
³⁵*University of London, Royal Holloway and Bedford New College, Egham, Surrey TW20 0EX, United Kingdom*
³⁶*University of Louisville, Louisville, Kentucky 40292, USA*
³⁷*Johannes Gutenberg-Universität Mainz, Institut für Kernphysik, D-55099 Mainz, Germany*
³⁸*University of Manchester, Manchester M13 9PL, United Kingdom*
³⁹*University of Maryland, College Park, Maryland 20742, USA*
⁴⁰*University of Massachusetts, Amherst, Massachusetts 01003, USA*
⁴¹*Massachusetts Institute of Technology, Laboratory for Nuclear Science, Cambridge, Massachusetts 02139, USA*
⁴²*McGill University, Montréal, Québec, Canada H3A 2T8*
^{46a}*INFN Sezione di Milano; I-20133 Milano, Italy*
^{46b}*Dipartimento di Fisica, Università di Milano, I-20133 Milano, Italy*
⁴³*University of Mississippi, University, Mississippi 38677, USA*
⁴⁴*Université de Montréal, Physique des Particules, Montréal, Québec, Canada H3C 3J7*
^{49a}*INFN Sezione di Napoli; I-80126 Napoli, Italy*
^{49b}*Dipartimento di Scienze Fisiche, Università di Napoli Federico II, I-80126 Napoli, Italy*
⁴⁵*NIKHEF, National Institute for Nuclear Physics and High Energy Physics, NL-1009 DB Amsterdam, The Netherlands*
⁴⁶*University of Notre Dame, Notre Dame, Indiana 46556, USA*
⁴⁷*Ohio State University, Columbus, Ohio 43210, USA*
⁴⁸*University of Oregon, Eugene, Oregon 97403, USA*
^{54a}*INFN Sezione di Padova; I-35131 Padova, Italy*
^{54b}*Dipartimento di Fisica, Università di Padova, I-35131 Padova, Italy*
⁴⁹*Laboratoire de Physique Nucléaire et de Hautes Energies, IN2P3/CNRS, Université Pierre et Marie Curie-Paris6, Université Denis Diderot-Paris7, F-75252 Paris, France*
^{56a}*INFN Sezione di Perugia; I-06100 Perugia, Italy*
^{56b}*Dipartimento di Fisica, Università di Perugia, I-06100 Perugia, Italy*
^{57a}*INFN Sezione di Pisa; I-56127 Pisa, Italy*
^{57b}*Dipartimento di Fisica, Università di Pisa; I-56127 Pisa, Italy*
^{57c}*Scuola Normale Superiore di Pisa, I-56127 Pisa, Italy*
⁵⁰*Princeton University, Princeton, New Jersey 08544, USA*
^{59a}*INFN Sezione di Roma; I-00185 Roma, Italy*
^{59b}*Dipartimento di Fisica, Università di Roma La Sapienza, I-00185 Roma, Italy*
⁵¹*Universität Rostock, D-18051 Rostock, Germany*
⁵²*Rutherford Appleton Laboratory, Chilton, Didcot, Oxon, OX11 0QX, United Kingdom*
⁵³*CEA, Irfu, SPP, Centre de Saclay, F-91191 Gif-sur-Yvette, France*
⁵⁴*SLAC National Accelerator Laboratory, Stanford, California 94309 USA*
⁵⁵*University of South Carolina, Columbia, South Carolina 29208, USA*
⁵⁶*Southern Methodist University, Dallas, Texas 75275, USA*
⁵⁷*Stanford University, Stanford, California 94305-4060, USA*
⁵⁸*State University of New York, Albany, New York 12222, USA*
⁵⁹*Tel Aviv University, School of Physics and Astronomy, Tel Aviv, 69978, Israel*
⁶⁰*University of Tennessee, Knoxville, Tennessee 37996, USA*
⁶¹*University of Texas at Austin, Austin, Texas 78712, USA*
⁶²*University of Texas at Dallas, Richardson, Texas 75083, USA*
^{72a}*INFN Sezione di Torino; I-10125 Torino, Italy*
^{72b}*Dipartimento di Fisica Sperimentale, Università di Torino, I-10125 Torino, Italy*
^{73a}*INFN Sezione di Trieste; I-34127 Trieste, Italy*
^{73b}*Dipartimento di Fisica, Università di Trieste, I-34127 Trieste, Italy*
⁶³*IFIC, Universitat de Valencia-CSIC, E-46071 Valencia, Spain*
⁶⁴*University of Victoria, Victoria, British Columbia, Canada V8W 3P6*
⁶⁵*Department of Physics, University of Warwick, Coventry CV4 7AL, United Kingdom*
⁶⁶*University of Wisconsin, Madison, Wisconsin 53706, USA*
(Received 24 May 2011; published 30 August 2011)

We search for CP violation in a sample of 20 000 Cabibbo-suppressed decays, $D^+ \rightarrow K^+ K_S^0 \pi^+ \pi^-$, and 30 000 Cabibbo-favored decays, $D_s^+ \rightarrow K^+ K_S^0 \pi^+ \pi^-$. We use 520 fb^{-1} of data recorded by the BABAR detector at the PEP-II asymmetric-energy $e^+ e^-$ collider operating at center of mass energies near 10.6 GeV. We search for CP violation in the difference between the T -odd asymmetries obtained

using triple product correlations of the D^+ (D_s^+) and D^- (D_s^-) decays, respectively. The T violation parameter values obtained are $\mathcal{A}_T(D^+) = (-12.0 \pm 10.0_{\text{stat}} \pm 4.6_{\text{syst}}) \times 10^{-3}$ and $\mathcal{A}_T(D_s^+) = (-13.6 \pm 7.7_{\text{stat}} \pm 3.4_{\text{syst}}) \times 10^{-3}$, which are consistent with the standard model expectations.

DOI: 10.1103/PhysRevD.84.031103

PACS numbers: 13.25.Ft, 11.30.Er

In the standard model (SM) of particle physics, the violation of the charge-conjugation and parity symmetries (CP) is introduced by the Kobayashi-Maskawa (KM) phase in the Cabibbo-Kobayashi-Maskawa quark mixing matrix [1]. The KM ansatz has been tested at high precision in K and B decays, where the KM phase contributes to the quark transition amplitude at tree level. However, further experimental efforts are needed in D meson decays, where CP -violating amplitudes are predicted to contribute to the observables at the 10^{-3} level [2].

The sensitivity to CP violation in D meson decays reached by the B factories is of the order of 5×10^{-3} [3–6]. Although this does not represent a measurement of SM CP violation, it provides a constraint on possible effects beyond the SM. New physics models introduce CP violation in D meson decays through tree and one-loop diagrams. While predictions for CP violation in tree diagrams are not different from those in the SM [$\mathcal{O}(10^{-3})$], new physics in loop diagrams may enhance CP violation effects at the order of 10^{-2} [7].

We report herein a search for CP violation in the decays $D^+ \rightarrow K^+ K_S^0 \pi^+ \pi^-$ and $D_s^+ \rightarrow K^+ K_S^0 \pi^+ \pi^-$ using T -odd correlations [8]. We define a kinematic triple product that is odd under time reversal using the vector momenta of the final state particles in the $D_{(s)}^+$ rest frame as

$$C_T \equiv \vec{p}_{K^+} \cdot (\vec{p}_{\pi^+} \times \vec{p}_{\pi^-}). \quad (1)$$

Under the assumption of CPT invariance, time-reversal (T) violation is equivalent to CP violation.

We study the T -odd correlations by measuring the observable expressed in Eq. (1) and then evaluating the asymmetry

$$A_T \equiv \frac{\Gamma(C_T > 0) - \Gamma(C_T < 0)}{\Gamma(C_T > 0) + \Gamma(C_T < 0)}, \quad (2)$$

where Γ is the decay rate for the process under study. The observable defined in Eq. (2) can have a nonzero value due to final state interactions, even if the weak phases are zero [9]. The T -odd asymmetry measured in the CP -conjugate decay process, \bar{A}_T , is defined as

$$\bar{A}_T \equiv \frac{\Gamma(-\bar{C}_T > 0) - \Gamma(-\bar{C}_T < 0)}{\Gamma(-\bar{C}_T > 0) + \Gamma(-\bar{C}_T < 0)}, \quad (3)$$

where $\bar{C}_T \equiv \vec{p}_{K^-} \cdot (\vec{p}_{\pi^-} \times \vec{p}_{\pi^+})$. We can then construct

$$\mathcal{A}_T \equiv \frac{1}{2}(A_T - \bar{A}_T), \quad (4)$$

which is an asymmetry that characterizes T violation in the weak decay process [10–12].

At least four different particles are required in the final state so that the triple product may be defined using momentum vectors only [13]. The D meson decays suitable for this analysis method are $D^+ \rightarrow K^+ K_S^0 \pi^+ \pi^-$, $D_s^+ \rightarrow K^+ K_S^0 \pi^+ \pi^-$, and $D^0 \rightarrow K^+ K^- \pi^+ \pi^-$. The search for CP violation using T -odd correlations in $D^0 \rightarrow K^+ K^- \pi^+ \pi^-$ has recently been carried out by the BABAR Collaboration, and no evidence of CP violation has been observed [3].

Following the suggestion by Bigi [14], the FOCUS Collaboration [15] first applied this technique to a sample of approximately 500 reconstructed D^+ and D_s^+ events, respectively. No evidence of CP violation was found. In the present analysis, we perform a similar measurement using approximately 2.1×10^4 D^+ and 3.0×10^4 D_s^+ meson decay candidates.

The analysis is based on a 520 fb^{-1} data sample recorded mostly at the $\Upsilon(4S)$ peak and at center of mass (CM) energy 40 MeV below the resonance by the BABAR detector at the PEP-II asymmetric-energy e^+e^- collider. Contributions to the data sample have been recorded near the $\Upsilon(3S)$ resonance ($\approx 31 \text{ fb}^{-1}$), and near the $\Upsilon(2S)$ resonance ($\approx 15 \text{ fb}^{-1}$). In addition, two large samples of Monte Carlo (MC) simulated events have been analyzed. In these samples, the $e^+e^- \rightarrow c\bar{c}$ production process is generated using JETSET 7.4 [16], and the detector response is simulated by GEANT 4 [17]. About 1.1×10^9 generic $e^+e^- \rightarrow c\bar{c}$ MC events, corresponding to 846 fb^{-1} , were generated to include the previously measured intermediate resonances in the $D_{(s)}^+$ decays, while 4.0×10^6 $e^+e^- \rightarrow D_{(s)}^+ X$ MC signal events ($\approx 1025 \text{ fb}^{-1}$), where X represents any system of charged and neutral particles compatible with the relevant conservation laws, were generated in which the $D_{(s)}^+$ signal decays to $K^+ K_S^0 \pi^+ \pi^-$ uniformly over the phase space. Both MC samples were processed using the same reconstruction and analysis chain as that used for real events.

The BABAR detector is described in detail elsewhere [18]. We mention here only the subsystems used in the present analysis. Charged-particle tracks are detected, and their momenta measured, with a combination of a cylindrical drift chamber (DCH) and a silicon vertex tracker (SVT), both operating within the 1.5-T magnetic field of a superconducting solenoid. The information from a ring-imaging Cherenkov detector, combined with specific energy-loss measurements in the SVT and DCH, provides identification of charged kaon and pion candidates.

The D^+ and D_s^+ meson decay candidates are reconstructed in the production and decay sequence:

$$e^+e^- \rightarrow XD_{(s)}^+; \quad D_{(s)}^+ \rightarrow K^+K_S^0\pi^+\pi^-; \quad K_S^0 \rightarrow \pi^+\pi^-, \quad (5)$$

using the events with at least five charged particles. We reconstruct $K_S^0 \rightarrow \pi^+\pi^-$ candidates using a vertex and kinematic fit with the K_S^0 mass constraint [19], and requiring a χ^2 probability greater than 0.1%. We accept only K_S^0 candidates that decay at least 0.5 cm from the e^+e^- interaction region (IR) and have a mass before the fit within 15 MeV/ c^2 of the nominal K_S^0 mass. The K_S^0 candidate is then combined with three charged-particle tracks with total net charge +1, to form a $D_{(s)}^+$ candidate. We require the tracks to originate from a common vertex, and the χ^2 fit probability (P_1) to be greater than 0.1%. In order to improve discrimination between signal and background, an additional fit is performed that constrains the three charged tracks to the IR. The χ^2 probability (P_2) of this fit is large for most of the background events, whose tracks originate from the IR, while it is smaller for $D_{(s)}^+$ signal events, whose tracks originate from a secondary vertex detached from the IR, due to the measurable $D_{(s)}^+$ flight distance. Particle identification is applied to the three charged-particle tracks, and the presence of a K^+ is required. Charged kaon identification has an average efficiency of 90% within the acceptance of the detector, and an average pion-to-kaon misidentification probability of 1.5%. We require the CM momentum of the $D_{(s)}^+$ candidate, p^* , to be greater than 2.5 GeV/ c . This requirement reduces the large combinatorial background from B decays, and improves the signal-to-background ratio significantly despite some loss in signal efficiency.

We first study backgrounds from charm meson decay processes which yield the same event topology.

The decay $D^{*+} \rightarrow \pi^+D^0$ produces a significant D^0 peak in the $K_S^0K^+\pi^-$ mass distribution. A fit with a Gaussian signal function yields a mass resolution of $\sigma_{D^0 \rightarrow K_S^0K^+\pi^-} = 4.6$ MeV/ c^2 . Selecting D^0 candidates within $\pm 3\sigma_{D^0 \rightarrow K_S^0K^+\pi^-}$ of the D^0 mass, we observe a clear D^{*+} peak in the distribution of the mass difference $\Delta m = m(K^+K_S^0\pi^+\pi^-) - m(K_S^0K^+\pi^-)$. This contribution is reduced to a negligible level by requiring $\Delta m > 0.1465$ GeV/ c^2 .

We also observe background from the decay $D^+ \rightarrow K^+K_S^0K_S^0$, with one of the K_S^0 decaying into the bachelor pions of Eq. (5). This contribution is removed by requiring the $\pi^+\pi^-$ invariant mass to lie outside a ± 8.7 MeV/ c^2 mass window around the nominal K_S^0 mass [19]. We look for backgrounds from $D^+ \rightarrow K_S^0\pi^+\pi^+\pi^-$ decays by assigning a pion mass hypothesis to the kaon candidate. We observe a D^+ signal over a large background. Simulation shows that this background produces a broad structure in the high-mass region of the D_s^+ mass distribution. We also looked for background from $\Lambda_c^+ \rightarrow pK_S^0\pi^+\pi^-$ decay by assigning the proton mass to the kaon candidate. We see a

signal over a large background. We find it impossible to remove the $D^+ \rightarrow K_S^0\pi^+\pi^+\pi^-$ and $\Lambda_c^+ \rightarrow pK_S^0\pi^+\pi^-$ events without biasing our mass distributions. Our MC simulations, however, show that the presence of these backgrounds does not bias the extraction of the $D_{(s)}^+$ meson yields. As a further check, we select a high purity data sample (87.5%) of $D^+ \rightarrow K_S^0\pi^+\pi^+\pi^-$ decays and assign the K^+ mass alternatively to both π^+ . We compute the asymmetries on the resulting integrated distributions and find that they are all consistent with zero. A similar result is obtained when we perform the test on MC events.

We divide the $K^+K_S^0\pi^+\pi^-$ mass spectrum into two regions in order to extract separately the D^+ and D_s^+ signal yields. For the former we require $1.81 < m(K^+K_S^0\pi^+\pi^-) < 1.92$ GeV/ c^2 , while for the latter we require $1.91 < m(K^+K_S^0\pi^+\pi^-) < 2.02$ GeV/ c^2 .

For further signal-to-background optimization, we explore three variables: the CM momentum, p^* , the difference in probability, $P_1 - P_2$, and the signed transverse decay length, $L_T = \frac{\vec{d} \cdot \vec{p}_T}{|\vec{p}_T|}$, where \vec{d} is the distance vector between the IR and the $D_{(s)}^+$ decay vertex in the transverse plane, and \vec{p}_T is the $D_{(s)}^+$ transverse momentum vector. Signal events are expected to be characterized by larger values of p^* [20], due to the jetlike topology of $e^+e^- \rightarrow c\bar{c}$ events, and larger values of L_T and $P_1 - P_2$, due to the measurable $D_{(s)}^+$ decay length.

Figure 1 shows the p^* , $P_1 - P_2$, and L_T distributions for signal and background in the D^+ and D_s^+ mass regions, respectively. The signal distributions are obtained from $D^+ \rightarrow K_S^0\pi^+\pi^+\pi^-$ and $D_s^+ \rightarrow K_S^0K^-\pi^+\pi^+$ decays in data after background subtraction. These decay modes are kinematically similar to the signal modes, but have higher signal yields and better signal-to-background ratios. The background distributions in Fig. 1 are obtained from $D_{(s)}^+ \rightarrow K^+K_S^0\pi^+\pi^-$ sidebands in the mass distributions for data.

The normalized probability distribution functions (\mathcal{P}) of the three variables for signal and background are combined in a likelihood-ratio test

$$\mathcal{L} = \prod_i \frac{\mathcal{P}_i^{\text{sig}}(x_i)}{\mathcal{P}_i^{\text{bkg}}(x_i)}, \quad \vec{x} = (p^*, P_1 - P_2, L_T) \quad (6)$$

to optimize the signal yields separately for D^+ and D_s^+ . The optimization of the cut is performed by maximizing the value of $S/\sqrt{S+B}$, where S is the number of signal events and $S+B$ is the total number of events in the signal region. The purity $S/(S+B)$ of the peak improves from 11.2% to 51.4% and from 16.6% to 60.6% for D^+ and D_s^+ , respectively.

Figure 2 shows the $K^+K_S^0\pi^+\pi^-$ mass spectra in the D^+ and D_s^+ regions before [(a) and (c)] and after [(b) and (d)] the likelihood-ratio test. For each region, the signal is described by the superposition of two Gaussian functions

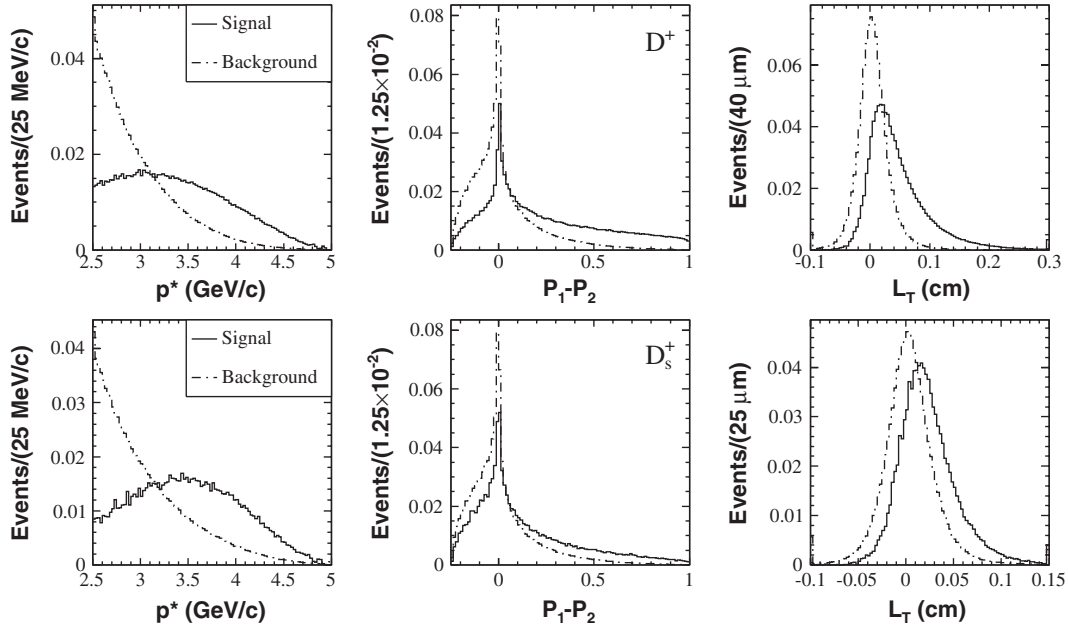


FIG. 1. Distributions of p^* , $P_1 - P_2$, and L_T for D^+ (top panels) and D_s^+ (bottom panels) candidates. The distributions for signal and background are shown as solid and dot-dashed histograms, respectively. All distributions are normalized to 1. Signal distributions are extracted from $D^+ \rightarrow K_S^0 \pi^+ \pi^-$ and $D_s^+ \rightarrow K_S^0 K^- \pi^+$ for D^+ and D_s^+ decays, respectively. The background distributions are extracted from the $D_{(s)}^+ \rightarrow K^+ K_S^0 \pi^+ \pi^-$ sidebands.

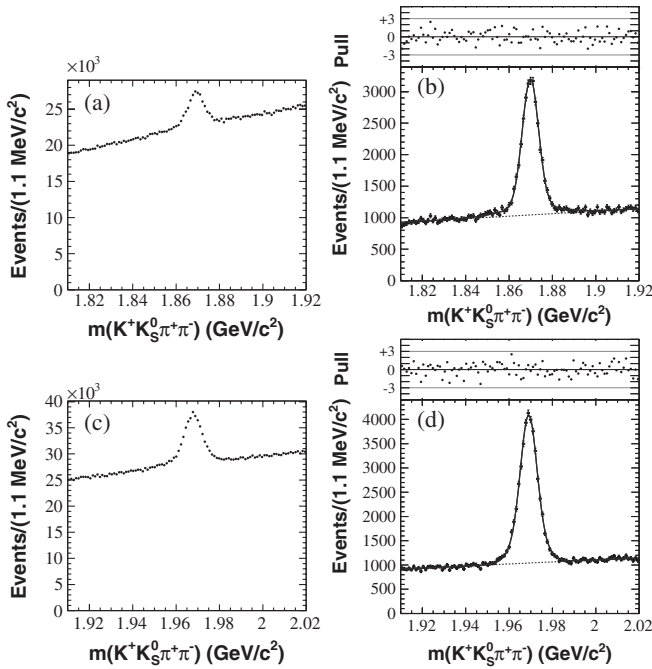


FIG. 2. The $K^+ K_S^0 \pi^+ \pi^-$ mass spectrum in the D^+ mass region (a) before and (b) after the cut on the likelihood ratio. Similar plots (c) and (d) are drawn for D_s^+ . The curves in (b) and (d) result from the fits described in the text. The distributions of the pull values are also shown. The χ^2/n_{dof} values from the fits are 0.87 (D^+) and 0.95 (D_s^+).

with a common mean value. The background is parametrized by a first-order polynomial in the D^+ region, and by a second-order polynomial in the D_s^+ region. The fitted functions are superimposed on the data in Fig. 2, and the fit residuals, shown above each distribution, are represented by $\text{Pull} = (N_{\text{data}} - N_{\text{fit}})/\sqrt{N_{\text{data}}}$. From these binned extended maximum likelihood fit, we extract the integrated yields $N(D^+) = 21\,210 \pm 392$ and $N(D_s^+) = 29\,791 \pm 337$ from the fits, where the uncertainties are statistical only. The mean value and width of the main Gaussian are $\mu_{D^+} = 1869.8 \pm 0.1 \text{ MeV}/c^2$, $\sigma_{D^+} = 3.76 \pm 0.08 \text{ MeV}/c^2$ for D^+ , and $\mu_{D_s^+} = 1969.0 \pm 0.1 \text{ MeV}/c^2$, $\sigma_{D_s^+} = 3.67 \pm 0.18 \text{ MeV}/c^2$ for D_s^+ .

We next divide the data sample into four subsamples depending on $D_{(s)}$ charge and whether C_T (\bar{C}_T) is greater or less than zero. We define

$$\begin{aligned}
 N(D_{(s)}^+, C_T > 0) &= \frac{N(D_{(s)}^+)}{2} (1 + A_T), \\
 N(D_{(s)}^+, C_T < 0) &= \frac{N(D_{(s)}^+)}{2} (1 - A_T), \\
 N(D_{(s)}^-, \bar{C}_T > 0) &= \frac{N(D_{(s)}^-)}{2} (1 - \bar{A}_T), \\
 N(D_{(s)}^-, \bar{C}_T < 0) &= \frac{N(D_{(s)}^-)}{2} (1 + \bar{A}_T),
 \end{aligned} \tag{7}$$

and fit the corresponding mass spectra simultaneously to extract the yields and the values of the asymmetry parameters A_T and \bar{A}_T . In this fit, the shape parameters are shared

among the four samples and are fitted together with the yields, $N(D_{(s)}^+)$ and $N(D_{(s)}^-)$, and the asymmetries, A_T and \bar{A}_T . The T -violating parameter \mathcal{A}_T is then computed using Eq. (4).

We validate the method by using the generic MC sample. We find that the fit results for A_T , \bar{A}_T , and the computed value of \mathcal{A}_T are in good agreement with those in the simulation, both for D^+ and D_s^+ .

All event selection criteria are determined before the final fit in order to avoid any potential bias. The true central values of A_T and \bar{A}_T are masked by adding unknown random offsets.

After removing the offsets, we measure the following asymmetries:

$$\begin{aligned} A_T(D^+) &= (+11.2 \pm 14.1_{\text{stat}} \pm 5.7_{\text{syst}}) \times 10^{-3}, \\ \bar{A}_T(D^-) &= (+35.1 \pm 14.3_{\text{stat}} \pm 7.2_{\text{syst}}) \times 10^{-3}, \end{aligned} \quad (8)$$

and

$$\begin{aligned} A_T(D_s^+) &= (-99.2 \pm 10.7_{\text{stat}} \pm 8.3_{\text{syst}}) \times 10^{-3}, \\ \bar{A}_T(D_s^-) &= (-72.1 \pm 10.9_{\text{stat}} \pm 10.7_{\text{syst}}) \times 10^{-3}. \end{aligned} \quad (9)$$

We observe values of A_T and \bar{A}_T which differ significantly from zero only for D_s^+ decay. This may indicate the presence of final-state-interaction effects for this decay process, perhaps as a result of the slightly different resonant substructure between D^+ and D_s^+ decay. For example, the $K^{*0}K^{*+}$ final state can contribute only to D_s^+ through a

doubly Cabibbo-suppressed decay process. In the case of D^+ decay we find A_T and \bar{A}_T to be consistent with zero, in contrast with the results of a similar analysis performed on the corresponding D^0 decay sample [3]:

$$\begin{aligned} A_T(D^0) &= (-68.5 \pm 7.3_{\text{stat}} \pm 5.8_{\text{syst}}) \times 10^{-3}, \\ \bar{A}_T(\bar{D}^0) &= (-70.5 \pm 7.3_{\text{stat}} \pm 3.9_{\text{syst}}) \times 10^{-3}. \end{aligned} \quad (10)$$

The fit results for the four data samples are shown in Figs. 3 and 4. Using Eq. (4) we obtain the T violation parameter values:

$$\mathcal{A}_T(D^+) = (-12.0 \pm 10.0_{\text{stat}} \pm 4.6_{\text{syst}}) \times 10^{-3} \quad (11)$$

and

$$\mathcal{A}_T(D_s^+) = (-13.6 \pm 7.7_{\text{stat}} \pm 3.4_{\text{syst}}) \times 10^{-3}. \quad (12)$$

For comparison, the value obtained for D^0 decay was [3]

$$\mathcal{A}_T(D^0) = (+1.0 \pm 5.1_{\text{stat}} \pm 4.4_{\text{syst}}) \times 10^{-3}. \quad (13)$$

The sources of systematic uncertainty considered in this analysis are listed in Table I, and were derived as follows:

- (1) We checked for possible asymmetries resulting from the detector response using large statistics signal MC samples in which the $D_{(s)}^+$ decays uniformly over phase space. These events are then weighted according to the resonant structures observed in the data (the resonances that contribute most are $\rho^0 \rightarrow \pi^+ \pi^-$, $K^{*0} \rightarrow K^+ \pi^-$, and $K^{*-} \rightarrow K_S^0 \pi^-$). Small variations with respect to the generated values

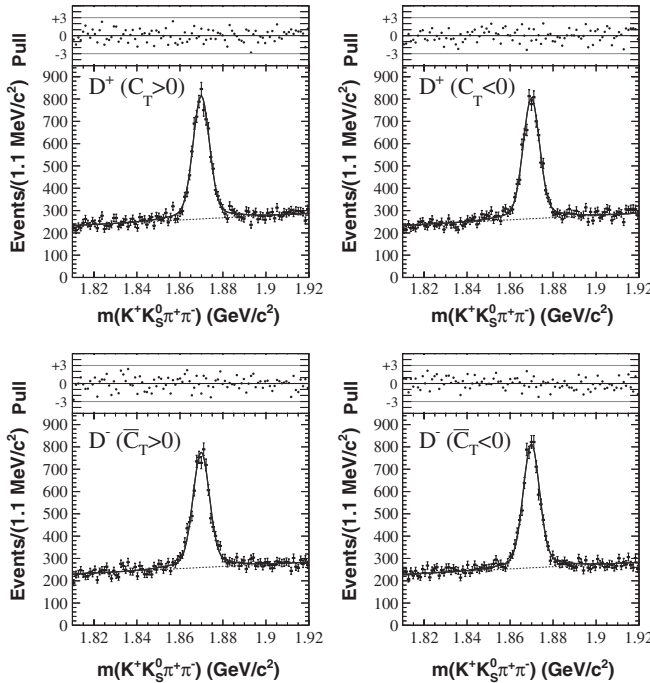


FIG. 3. Fits to the four $D^+ \rightarrow K^+ K_S^0 \pi^+ \pi^-$ data subsamples. The pull values are shown above each mass distribution. The χ^2/n_{dof} values from the fit are 1.07 (D^+ , $C_T > 0$), 1.10 (D^+ , $C_T < 0$), 1.19 (D^- , $\bar{C}_T > 0$), and 0.95 (D^- , $\bar{C}_T < 0$).

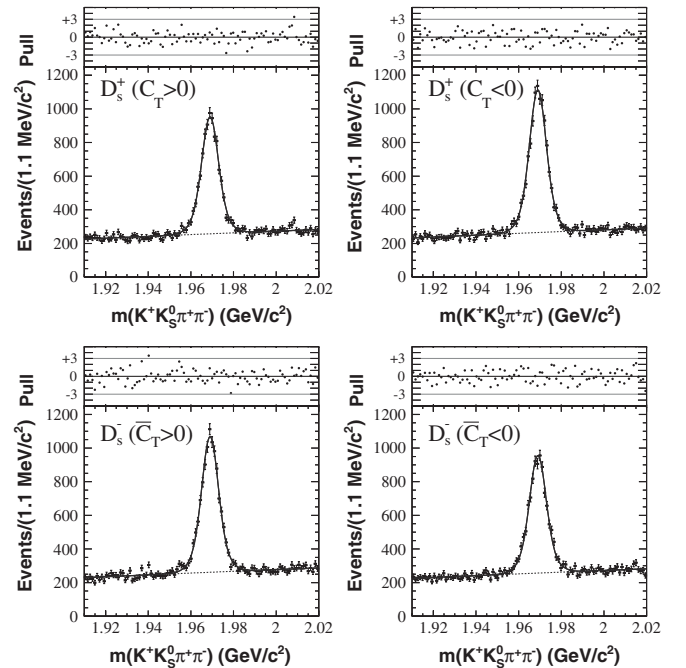


FIG. 4. Fits to the four $D_s^+ \rightarrow K^+ K_S^0 \pi^+ \pi^-$ data subsamples. The pull values are shown above each mass distribution. The χ^2/n_{dof} values from the fit are 1.05 (D_s^+ , $C_T > 0$), 1.03 (D_s^+ , $C_T < 0$), 1.15 (D_s^- , $\bar{C}_T > 0$), and 1.02 (D_s^- , $\bar{C}_T < 0$).

TABLE I. Systematic uncertainty evaluation for \mathcal{A}_T , A_T , and \bar{A}_T in units of 10^{-3} for $D^+ \rightarrow K^+ K_S^0 \pi^+ \pi^-$ and $D_s^+ \rightarrow K^+ K_S^0 \pi^+ \pi^-$.

Effect	$\mathcal{A}_T (D^+)$	$A_T (D^+)$	$\bar{A}_T (D^-)$	$\mathcal{A}_T (D_s^+)$	$A_T (D_s^+)$	$\bar{A}_T (D_s^-)$
(1) Reconstruction	2.1	2.8	1.3	0.7	1.0	1.3
(2) Likelihood ratio	1.1	3.4	5.6	2.5	7.8	8.2
(3) Fit model	1.3	1.1	1.5	0.1	0.8	0.7
(4) Particle identification	3.7	3.3	4.1	2.2	2.5	6.7
Total	4.6	5.7	7.2	3.4	8.3	10.7

are included in the evaluation of the systematic uncertainties. Using the same samples, we studied the effect of the forward-backward asymmetry caused by the interference between the electromagnetic current amplitude $e^+e^- \rightarrow \gamma^* \rightarrow c\bar{c}$ and the weak neutral current amplitude $e^+e^- \rightarrow Z^0 \rightarrow c\bar{c}$. This interference results in a $D_{(s)}^+/D_{(s)}^-$ production asymmetry that varies linearly with the cosine of the quark production angle θ^* , with respect to the e^- direction. Since the *BABAR* detector is asymmetric, the final $D_{(s)}^+$ and $D_{(s)}^-$ yields are not equal. To include this asymmetry in the MC samples, we weighted them for the $\cos\theta^*$ dependence measured in a previous analysis [4]. This study showed that the forward-backward asymmetry does not affect our measurements.

- (2) We modified the likelihood-ratio selection criteria, and considered the observed deviations from the central parameter values as sources of systematic uncertainty.
- (3) In order to check for final state radiation effects, we modified the fitting model by allowing the second Gaussian which describes the signal to have a free mean value. The background description was also modified by using higher order polynomials.
- (4) The particle identification algorithms used to identify kaons and pions were modified to more stringent or looser conditions in different combinations.

In the evaluation of the systematic uncertainty for each category, we keep the largest deviation from the reference

value, and assume that the uncertainty is symmetric. It should be noted that the systematic uncertainty on \mathcal{A}_T is not evaluated as the sum in quadrature of the errors on A_T and \bar{A}_T . Instead, it is evaluated directly from the deviation of \mathcal{A}_T resulting from the fits. This is why the error from the likelihood ratio or from particle identification is much smaller for \mathcal{A}_T than would be expected from the uncertainties on A_T and \bar{A}_T .

In conclusion, we have searched for *CP* violation using *T*-odd correlations in high statistics samples of Cabibbo-suppressed $D^+ \rightarrow K^+ K_S^0 \pi^+ \pi^-$ and Cabibbo-favored $D_s^+ \rightarrow K^+ K_S^0 \pi^+ \pi^-$ decays. We obtained *T*-violating asymmetries consistent with zero for both D^+ and D_s^+ decays with sensitivities of $\approx 1.0\%$ and $\approx 0.8\%$, respectively. We found that possible final-state-interaction effects in the $K^+ K_S^0 \pi^+ \pi^-$ final state are larger for D_s^+ decay than for D^+ decay.

We are grateful for the excellent luminosity and machine conditions provided by our PEP-II colleagues, and for the substantial dedicated effort from the computing organizations that support *BABAR*. The collaborating institutions wish to thank SLAC for its support and kind hospitality. This work is supported by DOE and NSF (USA), NSERC (Canada), CEA and CNRS-IN2P3 (France), BMBF and DFG (Germany), INFN (Italy), FOM (The Netherlands), NFR (Norway), MES (Russia), MICINN (Spain), and STFC (United Kingdom). Individuals have received support from the Marie Curie EIF (European Union), the A. P. Sloan Foundation (USA) and the Binational Science Foundation (USA-Israel).

-
- | | |
|--|---|
| <p>[1] N. Cabibbo, <i>Phys. Rev. Lett.</i> 10, 531 (1963); M. Kobayashi and T. Maskawa, <i>Prog. Theor. Phys.</i> 49, 652 (1973).</p> <p>[2] F. Buccella, M. Lusignoli, and A. Pugliese, <i>Phys. Rev. D</i> 51, 3478 (1995).</p> <p>[3] P. del Amo Sanchez <i>et al.</i> (<i>BABAR</i> Collaboration), <i>Phys. Rev. D</i> 81, 111103 (2010).</p> <p>[4] P. del Amo Sanchez <i>et al.</i> (<i>BABAR</i> Collaboration), <i>Phys. Rev. D</i> 83, 071103 (2011).</p> | <p>[5] B. R. Ko <i>et al.</i> (Belle Collaboration), <i>Phys. Rev. Lett.</i> 106, 211801 (2011).</p> <p>[6] B. R. Ko <i>et al.</i> (Belle Collaboration), <i>Phys. Rev. Lett.</i> 104, 181602 (2010).</p> <p>[7] Y. Grossman, A. L. Kagan, and Y. Nir, <i>Phys. Rev. D</i> 75, 036008 (2007).</p> <p>[8] The use of charge-conjugate reactions is implied throughout.</p> <p>[9] I. I. Bigi and H.-B. Li, <i>Int. J. Mod. Phys. A</i> 24, 657 (2009).</p> |
|--|---|

SEARCH FOR CP VIOLATION USING T -ODD . . .PHYSICAL REVIEW D **84**, 031103(R) (2011)

- [10] W. Bensalem, A. Datta, and D. London, *Phys. Rev. D* **66**, 094004 (2002).
- [11] W. Bensalem, A. Datta, and D. London, *Phys. Lett. B* **538**, 309 (2002).
- [12] W. Bensalem and D. London, *Phys. Rev. D* **64**, 116003 (2001).
- [13] E. Golowich and G. Valencia, *Phys. Rev. D* **40**, 112 (1989).
- [14] I.I. Bigi, Proceedings of KAON2001: International Conference on CP Violation, Pisa, Italy, 2001, p. 417.
- [15] J.M. Link *et al.* (FOCUS Collaboration), *Phys. Lett. B* **622**, 239 (2005).
- [16] T. Sjostrand, *Comput. Phys. Commun.* **82**, 74 (1994).
- [17] S. Agostinelli *et al.* (GEANT 4 Collaboration), *Nucl. Instrum. Methods Phys. Res., Sect. A* **506**, 250 (2003).
- [18] B. Aubert *et al.* (BABAR Collaboration), *Nucl. Instrum. Methods Phys. Res., Sect. A* **479**, 1 (2002).
- [19] K. Nakamura (Particle Data Group), *J. Phys. G* **37**, 075021 (2010).
- [20] B. Aubert *et al.* (BABAR Collaboration), *Phys. Rev. D* **65**, 091104 (2002).